Stem Cell Reports, Volume *14*

Supplemental Information

High-Resolution Dissection of Chemical Reprogramming from Mouse Embryonic Fibroblasts into Fibrocartilaginous Cells

Yishan Chen, Bingbing Wu, Junxin Lin, Dongsheng Yu, Xiaotian Du, Zixuan Sheng, Yeke Yu, Chengrui An, Xiaoan Zhang, Qikai Li, Shouan Zhu, Heng Sun, Xianzhu Zhang, Shufang Zhang, Jing Zhou, Varitsara Bunpetch, Ahmed El-Hashash, Junfeng Ji, and Hongwei Ouyang

Supplemental Materials

Supplemental data items

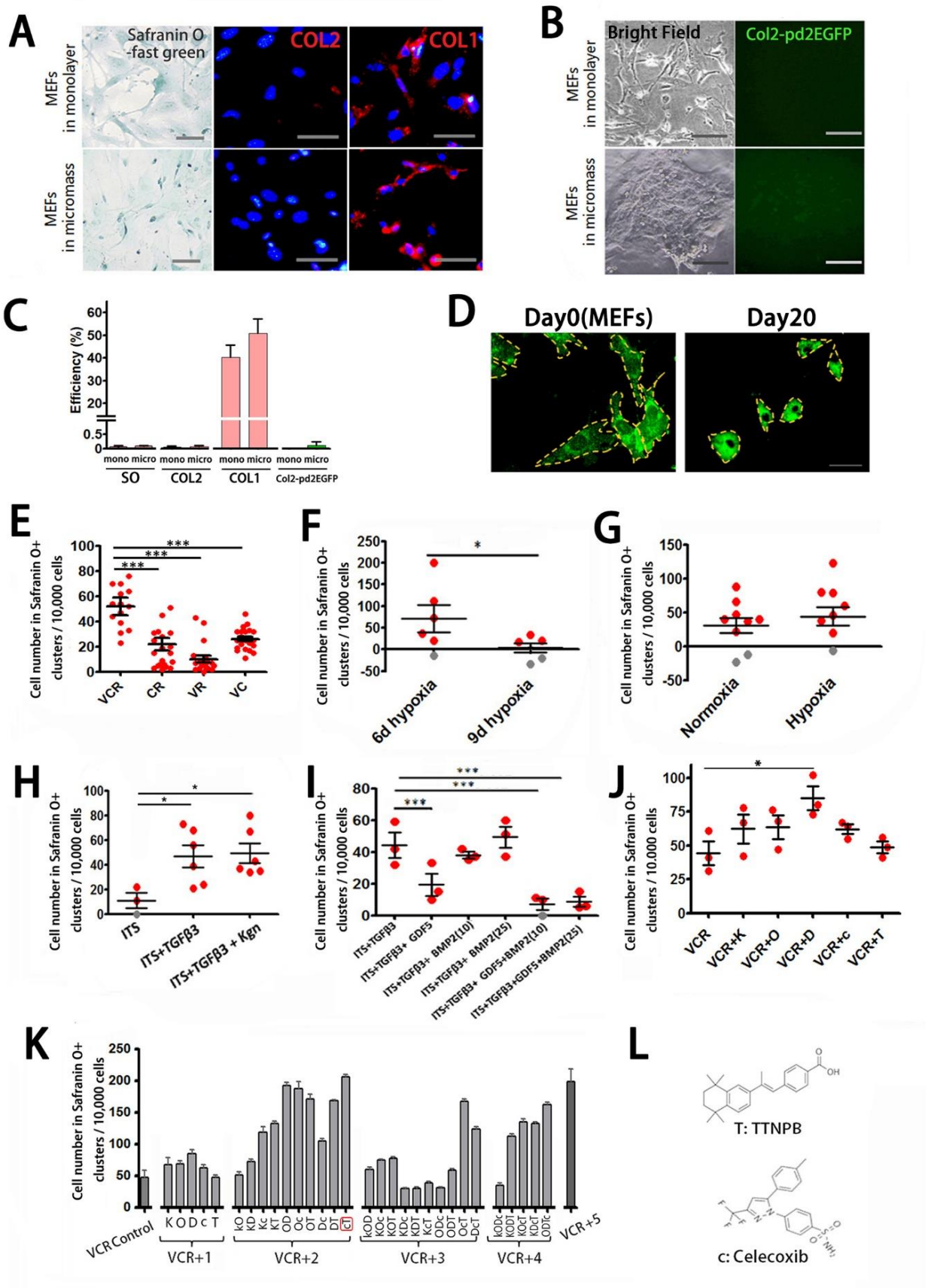
A
Safranin O
-fast green
COL2
COL1
MEFs
in monolayer
MEFs
in micromass
B
Bright Field
Col2-pd2EGFP
C
Efficiency (%)
mono micro
SO
COL2
COL1
Col2-pd2EGFP
D
Day0(MEFs)
Day20
E
Cell number in Safranin O+
clusters / 10,000 cells
VCR
CR
VR
VC
F
6d hypoxia
9d hypoxia
G
Normoxia
Hypoxia
H
ITS
ITS+TGFβ3
ITS+TGFβ3 + Kgn
I
ITS+TGFβ3
ITS+TGFβ3+ GDF5
ITS+TGFβ3+ BMP2(10)
ITS+TGFβ3+ BMP2(25)
ITS+TGFβ3+ GDF5+BMP2(10)
ITS+TGFβ3+GDF5+BMP2(25)
J
Cell number in Safranin O+
clusters / 10.000 cells
VCR
VCR+K
VCR+O
VCR+D
VCR+c
VCR+T
K
Cell number in Safranin O+
clusters / 10,000 cells
VCR Control
VCR+1
VCR+2
VCR+3
VCR+4
VCR+5
L
T: TTNPB
c: Celecoxib

Fig. S1. Efficient fibroblast-to-chondrocyte conversion using a chemical cocktail

(**A**) MEFs cultured in chondrogenic differentiation medium, stained by stained by Safranin O-fast greening, and immunostained by collagen type II (COL2) and collagen type I (COL1) antibodies; scale bars: 50 μm. (**B**) Col2-pd2EGFP fluorescence observation in MEFs directly cultured in chondrogenic differentiation medium; scale bars: 50 μm. (**C**) Quantitative data of Fig.S1A and B. Independent experiment, n=3. (**D**) Morphology changes of MEFs after chemical reprogramming (GFP-tagged cells); scale bars: 50 μm. (**E**) The contribution of individual compounds in cocktail VCR to fibroblast-to-chondrocyte conversion. Cell number in Safranin O^+ clusters was quantified on day 20. Independent experiment, n=3. (**F**) The optimization of induction time for Stage 1. Red dots represent cells in Safranin O+ clusters, while gray ones represent cells in Safranin O-/fast green+ clusters. (**G**) The contribution of hypoxia to fibroblast-to-chondrocyte induction. Independent experiment, n=3. (**H**)~(**I**) The optimization of chondrogenic factors in chondrogenic medium for Stage 2. TGFβ3：10ng/ml; BMP2 (10): 10ng/ml BMP2; BMP2 (25): 25ng/ml BMP2; GDF5: 10ng/ml. Kgn: Kartogenin. Independent experiment, n=3. (**J**) The primary screening of individual compound to identify 5 candidates: Kartogenin (K), Olanzapine (O), Dopamine HCl (D), Celecoxib (c) and TTNPB (T), treated together with VCR cocktail in Stage 1. Independent experiment, n=3. (**K**) The combinatory screening of 30 different combinations of 5 candidates together with VCR. VCR+1,2,3,4,5: VCR treatment together with individual compounds, or 2 or 3 or 4 or 5 compounds combined by K/O/D/c/T in Stage1. Independent experiment, n=3. (**L**) Chemical structure of TTNPB and Celecoxib, from www.selleckchem.com. Data are mean ± SEM, $n \geq 3$. *$p < 0.05$; **$p < 0.01$; ***$p < 0.001$. Related to Fig.1.

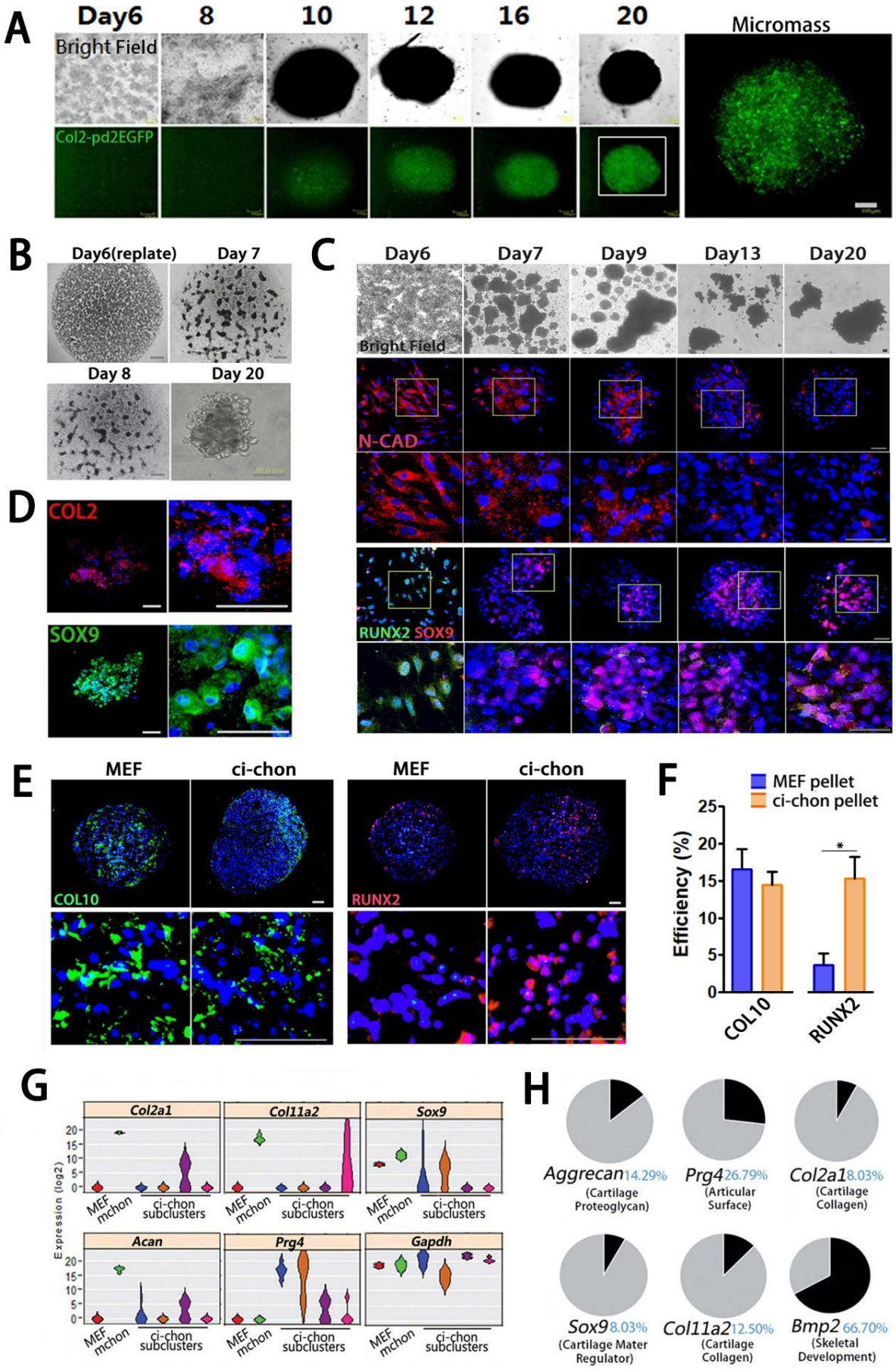
A
Day6
8
10
12
16
20
Micromass
Bright Field
Col2-pd2EGFP
B
Day6(replate)
Day 7
Day 8
Day 20
C
Day6
Day7
Day9
Day13
Day20
Bright Field
N-CAD
RUNX2 SOX9
D
COL2
SOX9
E
MEF
ci-chon
MEF
ci-chon
COL10
RUNX2
F
MEF pellet
ci-chon pellet
Efficiency (%)
25
20
15
10
5
0
*
COL10
RUNX2
G
Col2a1
Col11a2
Sox9
Acan
Prg4
Gapdh
Expression (log2)
20
15
10
5
0
MEF
mchon
ci-chon
subclusters
H
Aggrecan 14.29%
(Cartilage Proteoglycan)
Prg4 26.79%
(Articular Surface)
Col2a1 8.03%
(Cartilage Collagen)
Sox9 8.03%
(Cartilage Mater Regulator)
Col11a2 12.50%
(Cartilage Collagen)
Bmp2 66.70%
(Skeletal Development)

Fig. S2. Chemical-induced chondrocytes form scaffold-free cartilage organoids

(**A**) The real-time Col2-pd2EGFP observation in ci-chon micromass self-organized by VCRTc-treated MEFs, scale bars: 100 μm. (**B**) Chondro-like aggregations in micromass culture, scale bars: 500/50 μm. (**C**) Bright field images, immunostaining of N-Cadherin (N-CAD) and RUNX2/SOX9 of ci-chon pellets during Stage 2; scale bars: 50 μm. (**D**)Representative images of collagen type II (COL2) and SOX9 immunostaining of chondro-like aggregations, scale bars: 200 μm. (**E**)~(**F**) Immunostaining images of hypertrophic/osteoblast markers: COL10 and RUNX2 in MEF and ci-chon pellets and efficiency quantification; scale bars: 50μm. Independent experiment, n=3. (**G**) Violin plotting of the chondrogenic markers expressed in ci-chon subpopulations, analyzed by single cell qPCR. (**H**) Expression ratio of representative chondrocyte makers in ci-chons, analyzed by single cell qPCR data. Data are mean ± SEM, $n \geq 3$. *$p < 0.05$; **$p < 0.01$; ***$p < 0.001$. Related to Fig.2.

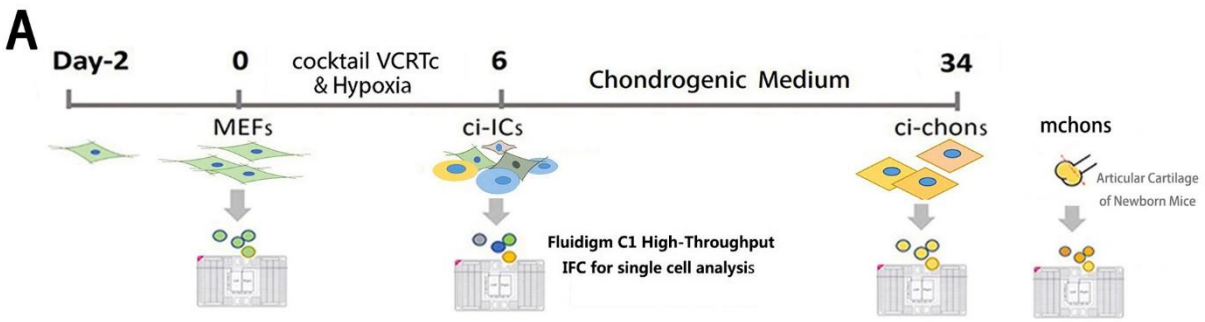
A
Day-2
0
cocktail VCRTc
& Hypoxia
6
Chondrogenic Medium
34
MEFs
ci-ICs
ci-chons
mchons
Articular Cartilage
of Newborn Mice
Fluidigm C1 High-Throughput
IFC for single cell analysis

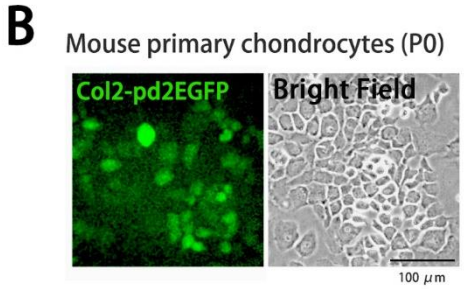
B
Mouse primary chondrocytes (P0)
Col2-pd2EGFP
Bright Field
100 μm


C
100%
80%
60%
40%
20%
0%
99.8%
81.01%
70%
30%
Cluster1
Cluster2
Cluster3
MEF
ci-IC
ci-chon
mchon

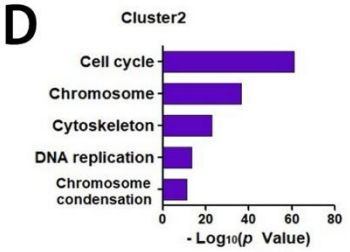
D
Cluster2
Cell cycle
Chromosome
Cytoskeleton
DNA replication
Chromosome condensation
0
20
40
60
80
- Log10(p Value)

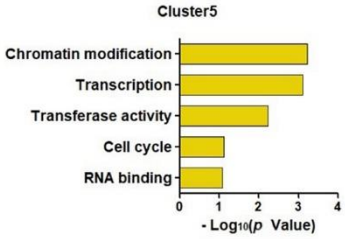
Cluster5
Chromatin modification
Transcription
Transferase activity
Cell cycle
RNA binding
0
1
2
3
4
- Log10(p Value)

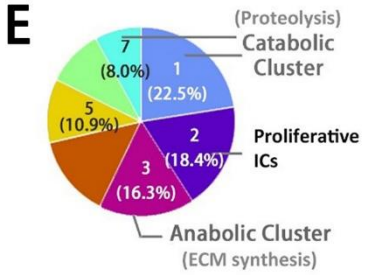
E
(Proteolysis)
Catabolic
Cluster
7
(8.0%)
1
(22.5%)
5
(10.9%)
2
(18.4%)
Proliferative
ICs
3
(16.3%)
Anabolic Cluster
(ECM synthesis)

Fig. S3. Single-cell transcriptomics of the fibroblast-to-chondrocyte reprogramming

(**A**) The strategy scheme of single cell RNA sequencing of 232 MEFs, 577 VCRTc-treated MEFs (also termed as chemical-induced intermediate cells (ci-ICs)); 311 chemical-induced chondrocytes (ci-chons), and 281 mouse primary chondrocytes (mchons). (**B**) Representative images of mouse primary articular chondrocytes (**C**) Cell type distribution in Cluster 1, 2 and 3. There are 91, 711, 400 cells in Cluster 1, 2, 3 respectively. (**D**) Enriched GO terms in Cluster 2 and 5, respectively marked by activation of proliferation and chromatin modification. (**E**) Pie diagram of cluster distribution of 7 ci-IC clusters. Related to Fig. 3 and 4.

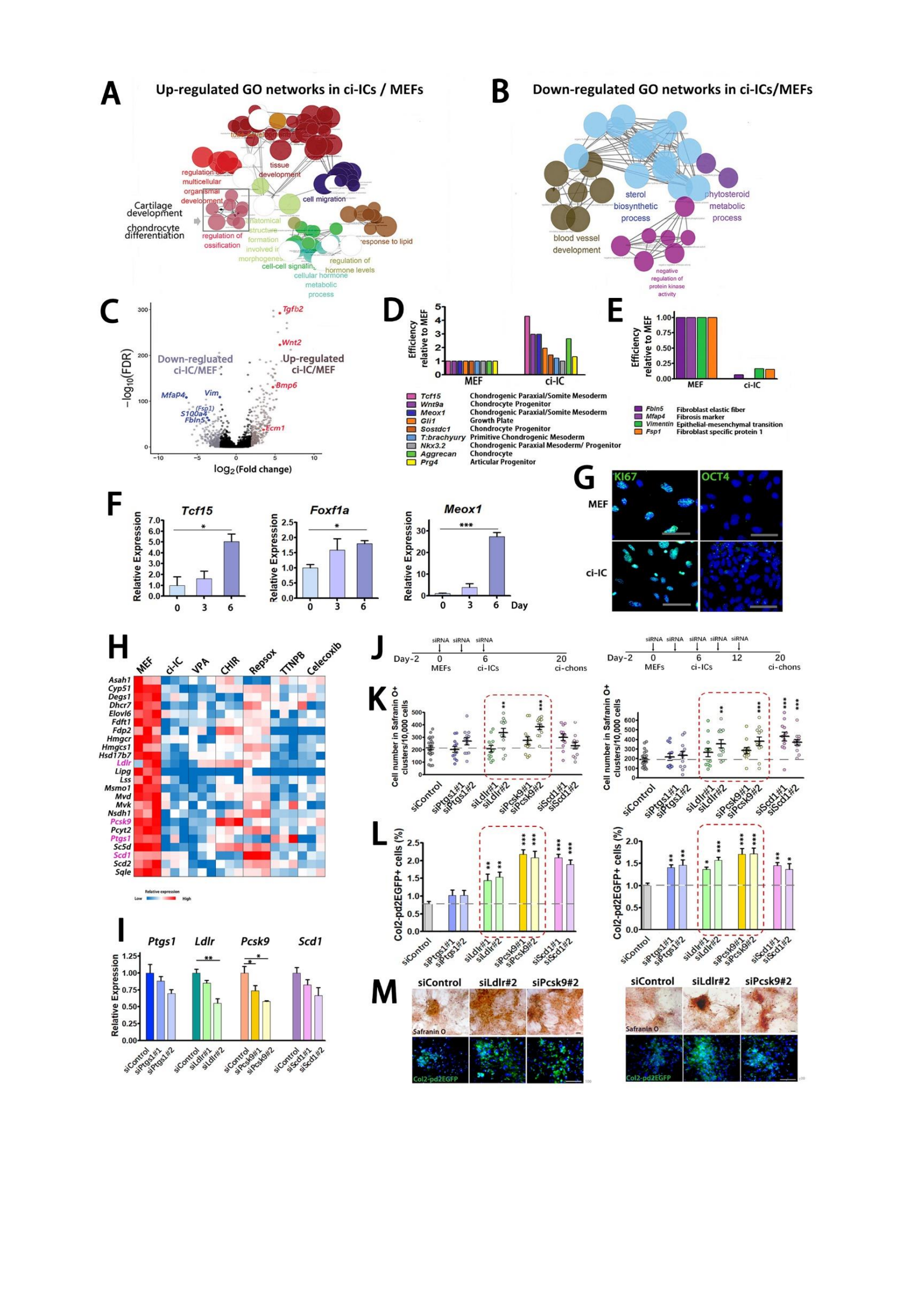
A
Up-regulated GO networks in ci-ICs / MEFs
tissue development
cell migration
Cartilage development
chondrocyte differentiation
regulation of ossification
response to lipid
regulation of hormone levels
B
Down-regulated GO networks in ci-ICs/MEFs
sterol biosynthetic process
phytosteroid metabolic process
blood vessel development
negative regulation of protein kinase activity
C
Down-regulated ci-IC/MEF
Up-regulated ci-IC/MEF
Tgfb2
Wnt2
Bmp6
Ecm1
Mfap4
Vim
S100a4
Fbln5
−log10(FDR)
log2(Fold change)
D
Efficiency relative to MEF
MEF
ci-IC
Tcf15 Chondrogenic Paraxial/Somite Mesoderm
Wnt9a Chondrocyte Progenitor
Meox1 Chondrogenic Paraxial/Somite Mesoderm
Gli1 Growth Plate
Sostdc1 Chondrocyte Progenitor
T:brachyury Primitive Chondrogenic Mesoderm
Nkx3.2 Chondrogenic Paraxial Mesoderm/ Progenitor
Aggrecan Chondrocyte
Prg4 Articular Progenitor
E
Efficiency relative to MEF
MEF
ci-IC
Fbln5 Fibroblast elastic fiber
Mfap4 Fibrosis marker
Vimentin Epithelial-mesenchymal transition
Fsp1 Fibroblast specific protein 1
F
Tcf15
Foxf1a
Meox1
Relative Expression
Day
G
KI67
OCT4
MEF
ci-IC
H
MEF
ci-IC
VPA
CHIR
Repsox
TTNPB
Celecoxib
Asah1
Cyp51
Degs1
Dhcr7
Elovl6
Fdft1
Fdp2
Hmgcr
Hmgcs1
Hsd17b7
Ldlr
Lipg
Lss
Msmo1
Mvd
Mvk
Nsdh1
Pcsk9
Pcyt2
Ptgs1
Sc5d
Scd1
Scd2
Sqle
Relative expression
Low
High
I
Ptgs1
Ldlr
Pcsk9
Scd1
Relative Expression
siControl
siPtgs1#1
siPtgs1#2
siLdlr#1
siLdlr#2
siPcsk9#1
siPcsk9#2
siScd1#1
siScd1#2
J
siRNA
Day-2
0
MEFs
6
ci-ICs
12
20
ci-chons
K
Cell number in Safranin O+ clusters/10,000 cells
L
Col2-pd2EGFP+ cells (%)
M
siControl
siLdlr#2
siPcsk9#2
Safranin O
Col2-pd2EGFP

Fig. S4. Fibroblast feature inhibition and chondrogenesis activation in early reprogramming

(**A**)~(**B**) GO networks of up-regulated and down-regulated genes in ci-ICs, relative to MEFs. (**C**) Volcano plot of representative markers up-regulated (red dots) and down-regulated (blue dots) in ci-ICs, relative to MEFs. (**D**)~(**E**) The relative expression ratio of cartilage developmental genes and fibroblast markers in ci-ICs, relative to MEFs, detected by single cell qPCR. (**F**) The time-dependent relative expression levels of osteochondral developmental genes during ci-ICs induction (Stage1), by bulk qPCR. Independent experiment, n=3. (**G**) Representative images of proliferative marker (KI67) and pluripotency marker (OCT4) immunostaining in MEFs and ci-ICs; scale bar: 50 μm. (**H**) Heatmap of representative fat metabolic genes in MEFs treated by individual compounds. (**I**) Knock down of representative fat metabolic genes (*Ptgs1*, *Ldlr*, *Pcsk9* and *Scd1*) by siRNAs, detected by qPCR. Scrambled siRNAs were used controls. Independent experiment, n=3. (**J**) Schematic diagram of screening strategy for siRNA inhibition. (**K**) Quantification of cell number in Safranin O^+ clusters, treated by VCRTc and siRNAs of *Ptgs1*, *Ldlr*, *Pcsk9* and *Scd1*. Independent experiment, n=3. (**L**) Percentage of Col2-pd2EGFP$^+$ cells, treated by VCRTc and siRNAs of *Ptgs1*, *Ldlr*, *Pcsk9* and *Scd1*. Independent experiment, n=3. (**M**) Representative images of Safranin O^+ clusters and Col2-pd2EGFP$^+$ cells in ci-chons treated by VCRTc and siRNAs of *Ldlr* and *Pcsk9*. Data are mean ± SEM, $n \geq 3$. *$p < 0.05$; **$p < 0.01$; ***$p < 0.001$. Related to Fig. 5.

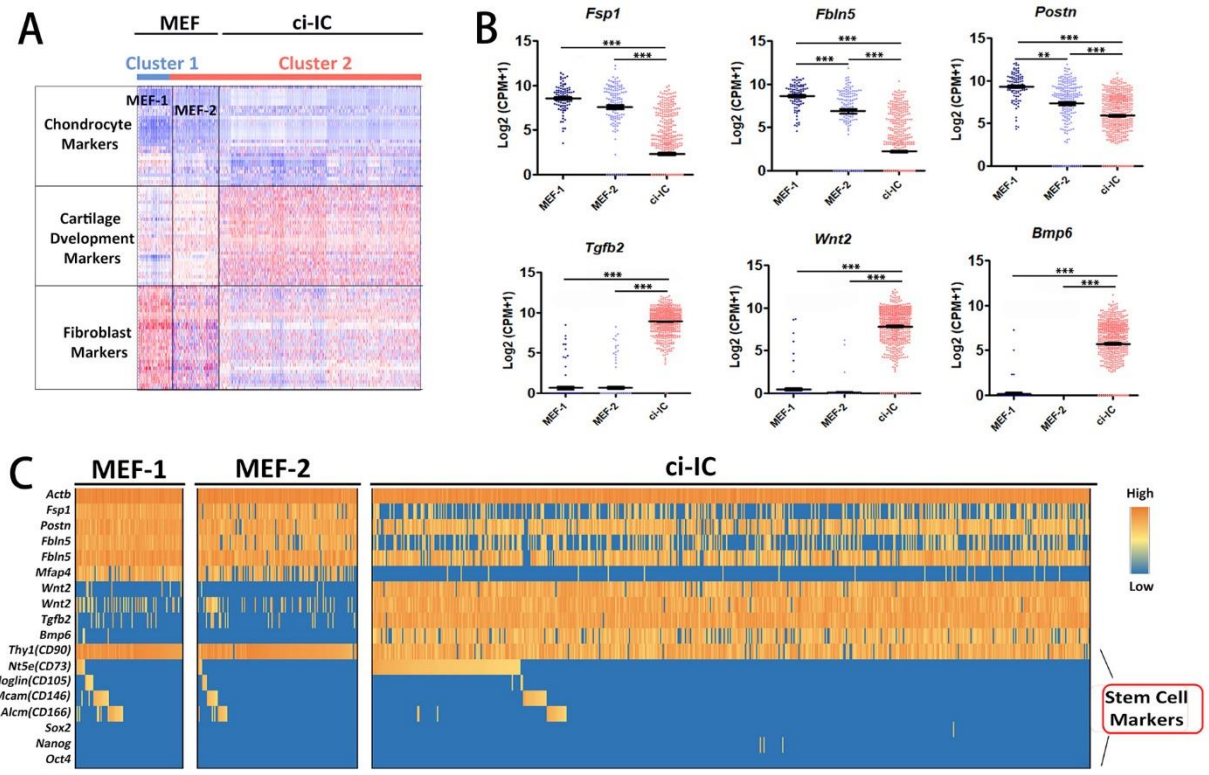

Fig. S5. The comparison of MEF subpopulations and ci-ICs

(**A**) Heatmap of cluster markers in MEF subpopulation MEF-1, MEF-2 and ci-ICs. See also in Seurat clustering of Fig.3C. (**B**) Relative expression levels of representative fibroblast and cartilage developmental markers in MEF-1, MEF-2 and ci-ICs. Data of single cell RNA sequencing. (**C**) Heatmap of fibroblast, cartilage developmental markers and stem cell markers in MEF-1, MEF-2 and ci-ICs. Data are mean ± SEM, n ≥ 3. *$p < 0.05$; **$p < 0.01$; ***$p < 0.001$. Related to Fig. 5.

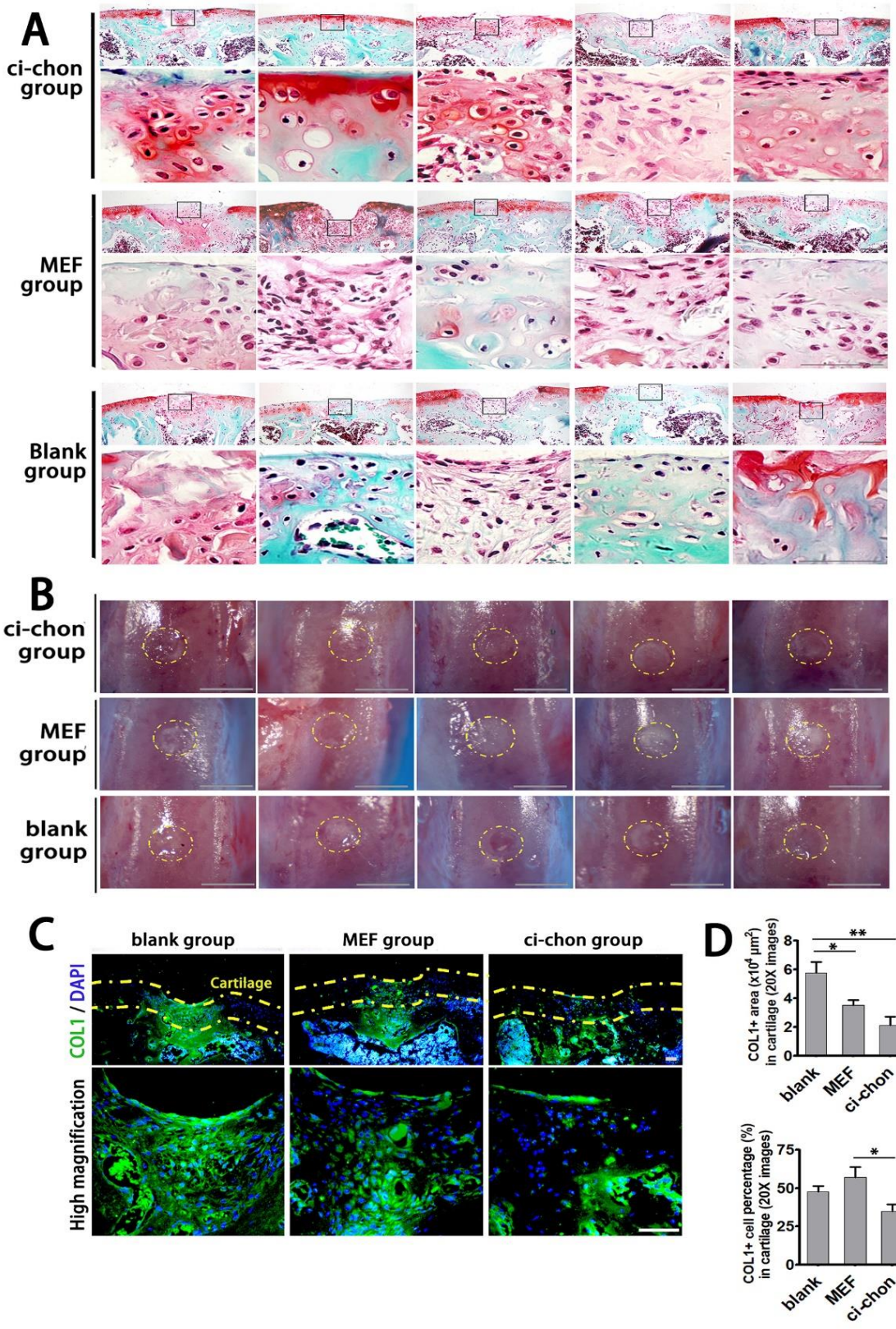
A
ci-chon group
MEF group
Blank group
B
ci-chon group
MEF group
blank group
C
blank group
MEF group
ci-chon group
COL1 / DAPI
Cartilage
High magnification
D
COL1+ area (x10⁴ μm²) in cartilage (20X images)
blank
MEF
ci-chon
COL1+ cell percentage (%) in cartilage (20X images)
blank
MEF
ci-chon

Fig. S6. *In vivo* cartilage regeneration by chemical-induced chondrocytes.

(**A**) Representative images of repaired articular surfaces in blank, MEF and ci-chon group (n = 5), stained by Safranin O-fast green. (**B**) Gross view of repaired articular surfaces in blank, MEF and ci-chon group (n = 5), scale bar: 500 μm. (**C**) Representative images of Safranin O-fast green staining and COL1 immunostaining in blank, MEF and ci-chon group (n=5); Safranin O-fast green staining was used to identify cartilage layer; scale bar: 50 μm. (**D**) Quantitative data of $COL1^+$ area and positive cell proportion in articular cartilage layer of blank, MEF and ci-chon group (n=5). Data are mean ± SEM, n ≥ 5. *$p < 0.05$; **$p < 0.01$; ***$p < 0.001$. *$p < 0.05$; **$p < 0.01$; ***$p < 0.001$. Related to Fig.6.

Table S1. Small molecules in primary screening

Name	Description	Concentration for Screening
Almotriptan Malate	5-hydroxytryptamine1B/1D receptor agonist	1μM
Ambroxol HCl	TTX-sensitive Na+ currents inhibitor	1μM
Amiloride HCl dihydrate	Epithelial sodium channel blocker	1μM
Azacitidine	DNA methylation inhbitor	1μM
Carvedilol	Beta blocker/alpha-1 blocker	1μM
Celecoxib	COX-2 inhibitor	1μM
Cyclopamine	Hedgehog (Hh) signaling pathway antagonist	1μM
Diphenidol HCl	AChR inhibitor	1μM
Dopamine	Neurotransmitter	1μM
Estriol	Antagonist of G-protein coupled estrogen receptor	1μM
Estrone	Estrogenic hormone	1μM
Ethisterone	Progestogen hormone	1μM
Exemestane	Aromatase inhibitor	1μM
Fluvastatin Sodium	HMG-CoA reductase inhibitor	1μM
Forskolin	Adenylyl cyclase agonist	1μM
Fulvestrant	Estrogen receptor (ER) antagonist	1μM
GO6983	PKC inhibitor	1μM
GSK343	H3K27me3 inhibitor	0.5μM
Hexestrol	ERxesRβRxestroloro	1μM
Honokiol	Akt-phosphorylation inhibitor	1μM
Imatinib	v-Abl, c-Kit inhibitor	1μM
Kartogenin	Chondrogenic inducer	0.1-0.2μM
Lafutidine	Histamine H(2)-receptor antagonist	1μM
Lansoprazole	Proton-pump inhibitor (PPI)	1μM
Letrozole	Aromatase inhibitor	1μM
Linifanib	VEGFR/PDGFR inhibitor	1μM
Lovastatin	HMG-CoA reductase inhibitor	1μM
LY294002	PI3K inhibitor	1μM
Manidipine 2HCl	Calcium channel blocker	1μM
Megestrol Acetate	Synthetic progesteronal agent	1μM
Milciclib (PHA-848125)	CDK inhibitor	1μM
NSC 23766	Rac1 inhibitor	1μM
Olanzapine	5-HT2 serotonin and D2 dopamine receptor	1μM
PD32591	MEK inhibitor	0.2μM
Raloxifene HCl	Estrogen antagonist	1μM
Ramipril	Angiotensin-converting enzyme (ACE) inhibitor	1μM
Rapamycin (Sirolimus)	mTOR inhibitor	1μM
Resveratrol	Sirtuin	1μM
Rolipram	PDE4-inhibitor	1μM
Rosiglitazone HCl	PPAR receptors inhibitor	1μM
Ruxolitinib	JAK1/2 inhibitor	1μM
SB203580	p38 MAPK inhibitor	1μM

Sodium Butyrate	HDAC inhibitor	2μM
SP600125	JNK inhibitor	2μM
Tranylcypromine	Monoamine oxidase inhibitor	1μM
TTNPB	(Arotinoid Acid) RAR agonist	1μM
Vitamin C	Vitamin	1μM
Y-27632	Rock inhibitor	1μM

Table S2. Candidate small molecules in combinatory screening

Name	**Description**	**Concentration (μM)**	**Catalog No.**
Kartogenin	Chondrogenic inducer	0.1	4513 (Tocris)
Olanzapine	5-HT2 serotonin and D2 dopamine receptor antagonist	1	S2493 (Selleck)
Dopamine HCl	Neurotransmitter	1	S2529 (Selleck)
Celecoxib	COX-2 inhibitor	1	S1261 (Selleck)
TTNPB	(Arotinoid Acid) RAR agonist	1	S4627 (Selleck)

Table S3. Representative markers for clusters containing MEFs, ci-ICs, ci-chons and mchons, by Seurat unbiased clustering

Table S4. Primers used in pre-amplification and single cell qPCR. Related to Fig. S2 and S5.

Supplementary Experimental Procedures

Cell isolation and culture. Primary MEFs were isolated from E13.5 embryos of wild-type C57BL/6J and Col2-pd2EGFP C57BL/6N mice, as previously described (Lujan et al.,2012). Briefly, the head, limbs, visceral tissues, gonads, vertebral column, rib and sternum were removed, and the remaining parts were cut into pieces, and then trypsinized. MEFs were maintained in high glucose Dulbecco's modified Eagle's medium (H-DMEM, Gibico), supplemented with 10% fetal bovine serum, 1 mM GlutaMax (Gibico) and 0.1 mM non-essential amino acid (NEAA, Invitrogen) at 37 °C with 5% CO2. MEFs of passage 1~3 were used for chemical induction and control. Mouse primary articular chondrocytes were isolated from the knees of newborn C57B6L/J mice (postnatal 0-4 days) (Salvat et al.,2005). Briefly, femoral condyles and tibial plateau were dislocated and the soft tissues and bone tissues were carefully discarded under a stereoscope. Then, we washed the collected cartilages with PBS and digested them with 0.1% collagenase II (Gibico) overnight (16 hours). After incubation, chondrocytes were collected by centrifuge and cultured in DMEM/F12 medium (Gibico), supplemented with 10% fetal bovine serum, at 37 °C with 5% CO_2. Chondrocytes of passage 0~1 (cultured no more than 48 hours) were used as positive controls for phenotype characterization. Mouse mesenchymal stem cell line (C3H/10T1/2) were purchased from the Cell Bank of the Chinese Academy of Sciences (Shanghai, China).

Drug screening for chondrogenic inducing cocktails. A two-stage basic model was adopted for the drug screening. Briefly, in 96-well plates, expanded MEFs (confluency 90%) were treated with cocktail VCR under a physiological hypoxia (5% O_2) during Stage1 (Day 0-6) and then cultured in chondrogenic differentiation medium during Stage2 (Day 6-20). In primary screening, we selected 48 small molecules (Table S1) that known to facilitate reprogramming, or regulate chondrogenesis from a chemical library (Selleck). Each compound was applied at either Stage1 or 2, respectively (96 conditions, Fig.1A). We identified 5 compounds (Table S2) as candidates in combinatory screening as they potentially improved reprogramming efficiency when applied in Stage 1(Fig. S1I). In the combinatory screening, we then tested 30 different combinations of these 5 candidates together with the VCR cocktail.

To have a quick quantification of conversion efficiency, we conducted Safranin O-fast green staining at the end of induction. Cells were fixed in in 4% (v/v) paraformaldehyde (PFA) solution for 20 min, and stained with fast-green (Sigma) for 30min and 0.1% Safranin O (Sigma) for 15 min at room temperature (RT).The photos of all Safranin O+ or fast green+ cell clusters in each well were taken by a microscope (Leica) (one 4X general image and 4~5 representative 20X images for each well). The cell number in Safranin O+ cell clusters were calculated for each well as the screening indicator. To confirm the results, MEFs of Col2a1-pd2EGFP mice were treated with cocktail VCRTc and cultured as described above. At the end of induction, cells were fixed in in 4% (v/v) PFA solution for 20 min, washed with PBS and visualized under a fluorescence microscope (Leica). We stained cell nuclei with DAPI to define the cell number.

Flow cytometry analysis. Pellets were digested with 0.2% collagenase (1:1 mixture of collagenase I/II, Gibico17100-017, 17101-105) for 1h at 37ºC, and then re-suspended as single cells in PBS. Col2-pd2EGFP MEFs and chemical-induced chondrocytes were analyzed and quantified by flow cytometry with a FACStar Plus Flow Cytometer (BD Biosciences). Wild-type MEFs without EGFP

served as negative control for gating. Data of 10,000 cells were collected for each samples, and FlowJo_V10 was used for data analysis.

Single cell qPCR. Individual cells were sorted into 96 well PCR plates. After centrifugation at 4 °C, the plates were immediately frozen on dry ice. Then, cell lyses and sequence-specific reverse transcription were performed using CellsDirect™One-Step qRT-PCR Kit (Thermo Fisher Scientific). Briefly, the wells were loaded with 5 μl CellsDirect 2X Reaction Mix, 0.2μl SuperScript III RT Platinum Taq Mix, 2.5μl 4X Primer Mix (200 nM) (Table S3) and 1.3μl Nuclease free H_2O. Then the plates were immediately placed on a PCR machine. The thermal cycling conditions were as follows: 50°C for 15min; 95°C for 2 min; (95°C for 15s + 60°C for 4min), 20 cycles; 4°C hold. The pre-amplification products were treated with Exonuclease I (New England BioLabs).

Next we mixed amplified /Exonuclease I treated samples with 2X SsoFast EvaGreen Supermix with Low ROX (Biorad), 20X DNA Bingding Dye Sample Loading Reagent (Fluidigm) and individual qPCR primers (Table S4), and performed qPCR programs using 96.96 Dynamic Arrays on a BioMark System (Fluidigm). Ct values were calculated using BioMark Real-Time PCR Analysis software (Fluidigm). A background Ct of 30 is used to generate Log2 scale gene expression levels for each gene. Data analysis were performed using SINGuLAR™Analysis Toolset 3.0 software (Fluidigm). PCA, hierarchical clustering, correlation, and visualization were performed according to the toolset by using the R software.

Single Cell RNA sequencing. Single cells were captured using Fluidigm™ C1 high-throughput IFC. Briefly, single cells were loaded on a microfluidic RNA-seq chip. We checked the cell number in each microfluidic chamber under a microscope, for further data exclusion of non-single-cell samples. Then cell lysis, reverse transcription and cDNA pre-amplification were performed on the chip according to Fluidigm's standard protocol. Illumina libraries were prepared by Illumina Nextera XT DNA Sample Preparation kit. Libraries were pooled and sequenced 150 bp paired-end on one lane of Illumina HiSeq xten. Raw sequencing reads was processed with Perl scripts to ensure the quality for further analysis. We first removed adaptor-polluted reads and low-quality reads. Then we discarded reads with number of N bases accounting for more than 5 %. The obtained clean data was mapped to the mm9 mouse genome release with bowtie2 (Langmead and Salzberg,2012). Reads for each gene were counted by HTSeq (Anders et al.,2015). After obtaining the digital gene expression (DGE) data matrix, we used Seurat for dimension reduction, clustering and differential gene expression analysis, following the publicly available guided tutorials (http://www.satijalab.org/seurat) (Macosko et al.,2015; Satija et al.,2015). R package Seurat was used for dimension reduction, clustering and differential gene expression analysis (Macosko et al.,2015; Satija et al.,2015). Briefly, we filtered out cells expressing <200 genes, resulting in 1202 cells expressing a total of 25495 genes. Dimensional reduction was performed with the high variable genes, and significant principle components ($p < 10^{-7}$) were used for unsupervised clustering. The FindAllMarkers function was then used to find the markers for each of the identified cell clusters. Gene ontology analysis was performed using DAVID (https://david.ncifcrf.gov/home.jsp) (Huang et al.,2009, 2009). R Bioconductor package Monocle (Trapnell et al.,2014) were used in cell clustering, and pseudo-time analysis. Briefly, single cell mRNA counts were loaded into Monocle as described by package releasers (http://www.bioconductor.org/packages/release/bioc/html/monocle.html). Genes expressed by less than 10 cells were excluded,

while qualified cells were chosen with total mRNA falling in mean ± 2sd. For cell clustering, genes expressed by over 5% of the qualified cells. Then, we ran reduceDimension function with t-SNE as the reduction method. Cell clusters were identified through density peak clustering, with each cell's local density (P) and nearest distance (Δ) threshold as 10. Subsequently, we adopted DDRTree method, orderCells function and plot_cell_trajectory function to reduce data dimensionality, order cells along pseudotime and visualize the result, respectively. Finally, the expression pattern along pseudotime of differentially expressed genes were printed through plot_pseudotime_heatmap and plot genes_in_pseudotime function.

Bulk RNA sequencing. RNA-seq was modified from a previous method (Picelli et al.,2013). Briefly, RNA was extracted from samples by Trizol reagent (TAKARA). Reverse transcription was conducted by SuperScript II reverse transcriptase (Invitrogen). Double strand cDNA was conducted using NEBNext mRNA second strand synthesis kit (NEB) and then cleaned with AMPure XP beads (Beckman Coulter). 3'end enriched sequencing library was constructed with Nextera XT kit (Illumina) and sequenced on Illumina X-Ten platform. Raw sequencing reads was processed with Perl scripts to ensure the quality for further analysis. We first removed adaptor-polluted reads and low-quality reads. Then we discarded reads with number of N bases accounting for more than 5 %. The obtained clean data was mapped to the mm9 mouse genome release with bowtie2 (Langmead and Salzberg,2012). Reads for each gene were counted by HTSeq (Anders et al.,2015). After obtaining the gene expression data matrix, differential expression genes were analyzed with DESeq2 using count data of each gene (Love et al.,2014). Differential expression genes with p <0.05 were selected for further gene ontology analysis. Gene ontology and KEGG pathway analysis was performed using DAVID (https://david.ncifcrf.gov/home.jsp) (Huang et al.,2009, 2009).

Animals. Embryonic (E13.5) and newborn (0-4 days) wild type C57BL/6J mice for primary MEF and chondrocyte isolation, adult (8 weeks old) wild type C57BL/6J mice for full thickness cartilage defects animal model, and tdTomato mice (B6.129 (Cg)-Gt(ROSA)26Sortm4(ACTB-tdTomato,-EGFP)Luo/J) for cell tracing were purchased from Model Animal Research Center of Nanjing University (MARC). Col2-pd2EGFP reporter mice were gifted by William A. Hortonfrom Oregon Health and Science University.

***In vivo* implantation.** Full thickness cartilage defect operation was performed similar with previous studies (Eltawil et al.,2009; Wang et al.,2017) .8-week-old C57BL/6J mice were anesthetized with sodium pentobarbital (8mg/ml in 0.9% saline, 0.1ml/10g). Then the joint area was shaved and a 1cm skin incision was made on the medial side of the knee. We opened the joint capsule, performed the luxation of patellar ligament to expose the femoral trochlear groove of femur. A circular defect was made in the middle of the trochlear groove using a 30G (0.3mm) needle. The defect thickness was confirmed with bleeding in the defect hole after removing the needle. At last the ci-chon pellets (2×10^5 cells) were transplanted into the defect. After surgery, mice were placed in a clean cage on a heated pad to recover and were then housed for 6 weeks before collection of the joints. For sham group, we opened the joint capsule, but did not make the full thickness cartilage defect. For blank group, the full thickness cartilage defect operation was performed without tissue transplantation. For MEF group, MEF (2×10^5 cells) pellets were implanted. All animal

experiments were approved by the Zhejiang University Ethics Committee (ZJU20170786). The treatment was randomized and blinded from team members who performed the surgeries, postsurgical care and histological scoring.

Histological processing and analysis. Pellets (n=3 for each group) were harvested and fixed with 4% PFA for over 24h at RT. Then the samples were dehydrated through an alcohol gradient and embedded in paraffin blocks. Histological sections (5 μm) were prepared for the whole pellet using a microtome (Leica). For each sample, we collected 80~100 continuous sections. Three representative sections on the middle level were chosen for immunostaining. Mouse joint samples (n=5 for each group) of cartilage defect model were harvested and fixed with 4% PFA for over 48h at RT. Then the samples were decalcified in neutral 10% EDTA solution for 1 month at RT. Subsequently, they were dehydrated through an alcohol gradient and embedded in paraffin blocks. Histological sections (7 μm) were prepared using a microtome (Leica). For each sample, we collected 80~100 continuous sections. Six representative sections on the middle level were chosen for further analysis. For Safranin O-fast green staining, paraffin sections were stained with fast-green (Sigma) for 8 min and Safrannin O (Sigma) for 5 min at RT. We used ICRS II scoring system (Mainil-Varlet et al.,2010) to quantify cartilage histological restoration. Briefly, the scoring was conducted based on ICRS II method by 4 independent individuals, who were blinded to the group information. 13 parameters related to regenerative features (tissue morphology, matrix staining, cell morphology, chondrocyte clustering, architecture of surface, basal integration, formation of tidemark, subchondral bone fibrosis, inflammation, abnormal calcification, vascularization, surface/superficial assessment, and mid/deep zone assessment) plus overall assessment were scored by a 100-mm visual analog scale. Thus, a score of 0 was assigned for poor quality and 100 for good-quality/healthy cartilage.

Immunofluorescence staining. For immunofluorescence staining, cells cultured on glass coverslips were fixed in 4% (v/v) PFA solution for 20 min, then incubated in 0.3% Triton X-100 for 10min at RT, and incubated in 1% bovine serum albumin blocking buffer for 30 min at (RT). Afterwards, samples were incubated with primary antibodies at 4 °C overnight, and then with appropriate fluorescent probe-conjugated secondary antibodies for 2 hours at RT. Cell nuclei were counterstained with DAPI. Images were taken by confocal microscopy (Zeiss).

Specific primary antibodies used include COL2 (1:100, Millipore, MAB1330), Sox9 (1:100, abcam, ab76997), ACAN (1:50, Santa Cruz, sc-25674), PRG4/LUBRICIN (1:200, Abcam, ab28484), Col1a1 (1:50, Santa Cruz, SC-8784-R), Anti-RFP (1:100, Abcam, ab62341), ALexar Fluor 546 phalloidin (1:50, Invirogen, A22283).

AFM-based nanoindentation. Before the mechanical test, articular tissue samples were maintained in 4°C PBS no longer than 24h to minimize post-mortem degradation. AFM-based nanoindentation was performed on the recovered surfaces of femoral trochlear groove cartilage. Nanostiffness mapping was performed with Piuma nanoindentation according to the manufacturer's protocol, and the stiffness range of the cantilever is 1~5N/m. At least 3 samples were used for each group, and more than 5 locations were chosen to detect within 30μm around the defect center for each sample. The effective indentation modulus, Eind, was calculated by fitting the loading portion of each F-D curve to the Hertz model (Doyran et al.,2017).

Supplemental References

Anders, S., Pyl, P.T. and Huber, W. (2015). HTSeq--a Python framework to work with high-throughput sequencing data. Bioinformatics 31, 166-169.

Doyran, B., Tong, W., Li, Q., Jia, H., Zhang, X., Chen, C., Enomoto-Iwamoto, M., Lu, X.L., Qin, L. and Han, L. (2017). Nanoindentation modulus of murine cartilage: a sensitive indicator of the initiation and progression of post-traumatic osteoarthritis. Osteoarthritis Cartilage 25, 108-117.

Eltawil, N.M., De Bari C, Achan, P., Pitzalis, C. and Dell'accio, F. (2009). A novel in vivo murine model of cartilage regeneration. Age and strain-dependent outcome after joint surface injury. Osteoarthritis Cartilage 17, 695-704.

Huang, d.W., Sherman, B.T. and Lempicki, R.A. (2009). Bioinformatics enrichment tools: paths toward the comprehensive functional analysis of large gene lists. Nucleic Acids Res 37, 1-13.

Huang, d.W., Sherman, B.T. and Lempicki, R.A. (2009). Systematic and integrative analysis of large gene lists using DAVID bioinformatics resources. Nat Protoc 4, 44-57.

Langmead, B. and Salzberg, S.L. (2012). Fast gapped-read alignment with Bowtie 2. Nat Methods 9, 357-359.

Love, M.I., Huber, W. and Anders, S. (2014). Moderated estimation of fold change and dispersion for RNA-seq data with DESeq2. Genome Biol 15, 550.

Lujan, E., Chanda, S., Ahlenius, H., Südhof, T.C. and Wernig, M. (2012). Direct conversion of mouse fibroblasts to self-renewing, tripotent neural precursor cells. Proc Natl Acad Sci U S A 109, 2527-2532.

Macosko, E.Z., Basu, A., Satija, R., Nemesh, J., Shekhar, K., Goldman, M., Tirosh, I., Bialas, A.R., Kamitaki, N., Martersteck, E.M., et al. (2015). Highly Parallel Genome-wide Expression Profiling of Individual Cells Using Nanoliter Droplets. Cell 161, 1202-1214.

Mainil-Varlet, P., Van Damme B, Nesic, D., Knutsen, G., Kandel, R. and Roberts, S. (2010). A new histology scoring system for the assessment of the quality of human cartilage repair: ICRS II. Am J Sports Med 38, 880-890.

Picelli, S., Björklund, Å.K., Faridani, O.R., Sagasser, S., Winberg, G. and Sandberg, R. (2013). Smart-seq2 for sensitive full-length transcriptome profiling in single cells. Nat Methods 10, 1096-1098.

Salvat, C., Pigenet, A., Humbert, L., Berenbaum, F. and Thirion, S. (2005). Immature murine articular chondrocytes in primary culture: a new tool for investigating cartilage. Osteoarthritis Cartilage 13, 243-249.

Satija, R., Farrell, J.A., Gennert, D., Schier, A.F. and Regev, A. (2015). Spatial reconstruction of single-cell gene expression data. Nat Biotechnol 33, 495-502.

Trapnell, C., Cacchiarelli, D., Grimsby, J., Pokharel, P., Li, S., Morse, M., Lennon, N.J., Livak, K.J., Mikkelsen, T.S. and Rinn, J.L. (2014). The dynamics and regulators of cell fate decisions are revealed by pseudotemporal ordering of single cells. Nat Biotechnol 32, 381-386.

Wang, J., Zhang, F., Tsang, W.P., Wan, C. and Wu, C. (2017). Fabrication of injectable high strength hydrogel based on 4-arm star PEG for cartilage tissue engineering. Biomaterials 120, 11-21.